Received: 10 June 2020 | Revised: 5 August 2020 | Accepted: 8 August 2020

DOI: 10.1002/nbm.4400

Check for updates

RAPID COMMUNICATION

NMR IN BIOMEDICINE WILEY

Localized singlet-filtered MRS in vivo

Salvatore Mamone[1,2] | Andreas B. Schmidt[3,4,5] | Niels Schwaderlapp[3] | Thomas Lange[3] | Dominik von Elverfeldt[3] | Jürgen Hennig[3] | Stefan Glöggler[1,2]

[1]NMR Signal Enhancement Group, Max Planck Institute for Biophysical Chemistry, Göttingen, Germany

[2]Center for Biostructural Imaging of Neurodegeneration of UMG, Göttingen, Germany

[3]Department of Radiology, Medical Physics, Medical Center—University of Freiburg, Faculty of Medicine, University of Freiburg, Freiburg, Germany

[4]German Consortium for Cancer Research (DKTK), partner site Freiburg, Freiburg, Germany

[5]German Cancer Research Center (DKFZ), Heidelberg, Germany

Correspondence
Stefan Glöggler, NMR Signal Enhancement Group, Max Planck Institute for Biophysical Chemistry, Am Faßberg 11, 37077 Göttingen, Germany.
Email: stefan.gloeggler@mpibpc.mpg.de

Funding information
German Consortium for Translational Cancer Research; Max-Planck-Gesellschaft

MR is a prominent technology to investigate diseases, with millions of clinical procedures performed every year. Metabolic dysfunction is one common aspect associated with many diseases. Thus, understanding and monitoring metabolic changes is essential to develop cures for many illnesses, including for example cancer and neurodegeneration. MR methodologies are especially suited to study endogenous metabolites and processes within an organism in vivo, which has led to many insights about physiological functions. Advancing metabolic MR techniques is therefore key to further understand physiological processes. Here, we introduce an approach based on nuclear spin singlet states to specifically filter metabolic signals and particularly show that singlet-filtered glutamate can be observed distinctly in the hippocampus of a living mouse in vivo. This development opens opportunities to make use of the singlet spin phenomenon in vivo and besides its use as a filter to provide scope for new contrast agents.

KEYWORDS

brain, in vivo, magnetic resonance, metabolites, MRS, singlet state, spectroscopy

1 | INTRODUCTION

Metabolic imaging is a field of research that offers insights into metabolic pathways to understand the organism's function and the development of diseases and to evaluate clinical conditions. To this end, magnetic resonance spectroscopy (MRS), which is based on the nuclear magnetic resonance (NMR) phenomenon, is a versatile method to monitor endogenous molecules. Often, a large proton background arising from water and other more abundant molecules, in combination with limited spectral dispersion and poor homogeneity, obscures the observation of specific metabolites in MRS. A key challenge in the field is therefore to filter in vivo specific metabolites that are of interest and may serve as biomarkers for diseases.[1–7] Prominent examples of molecules are glutamine, glutamate, N-acetyl aspartate (NAA) and glutathione (GSH), which are essential for the brain metabolism.[5–7] In this article, we are introducing a localized metabolic approach using a spin phenomenon that has not yet been exploited in the context of (in vivo) MRS yet: nuclear spin singlet states. Singlet states are spin-0 states, formed by coupled spin-1/2 pairs that are

Abbreviations: CHESS, chemically selective saturation; gc-M2S, general-condition magnetization-to-singlet technique; ge-STF, gradient enhanced spherical tensor filter; GSH, glutathione; M2S, magnetization-to-singlet technique; NAA, N-acetyl aspartic acid; OVS, outer volume suppression; PBS, phosphate-buffered saline; PRESS, point resolved spectroscopy; SiFi-MRS, singlet-filtered MRS; SQ, single quantum; STO, spherical tensor operator; ZQ, zero quantum.

This is an open access article under the terms of the Creative Commons Attribution-NonCommercial-NoDerivs License, which permits use and distribution in any medium, provided the original work is properly cited, the use is non-commercial and no modifications or adaptations are made.
© 2020 The Authors. NMR in Biomedicine published by John Wiley & Sons Ltd

NMR silent. However, they can be probed indirectly.[8,9] A special feature of the singlet states is that their equilibration time (T_S) with the thermodynamically favored triplet states relaxes differently compared with the longitudinal relaxation T_1.[8–12] The latter represents the time that spins in the triplet case require to return to their thermodynamic equilibrium and also reflects the molecular dynamics, which makes T_1 an important contrast mechanism for MRI. As a result, and based on different relaxation effects on T_S, singlet states may add additional dimensions for studying diseases. One aspect of interest is the development of contrast agents based on the observation that T_S can be several times longer than T_1. A promising application is to pair prolonged lifetimes with prospective hyperpolarized contrast agents, where the NMR signals are enhanced by several orders of magnitude.[13–19] Large signal enhancements are successfully achieved and used—but currently without singlet states—in the medical context for imaging exogenous and ^{13}C-enriched metabolites such as pyruvate and to assess their metabolic conversion in, eg, tumors.[16–19] The traceability of such compounds is limited to about 2-3 min due to a short T_1. Singlet states have the potential to significantly extend this time, as a T_S in excess of 1 h has been reported for specifically designed molecules.[20]

The use of singlet states in MRI has been demonstrated for studying flow and diffusion in highly concentrated (∼1 M) doubly ^{13}C labelled compounds dissolved in organic solvent, where the singlet bearing spin pair is almost isolated and in conditions of strong coupling, using a microimaging system at 11.7 T.[21] However, these conditions are not the common occurrence for metabolites in vivo, which are dissolved in water at less than 10 mM concentrations, and in which singlet states have to be accessed in ^{1}H multi-spin systems, which span a variety of coupling regimes. Singlet states offer the possibility to selectively filter the signal from specific metabolites. Once a singlet state is populated, other coherences can be suppressed, and upon converting the singlet states back into an observable state only the signal of interest is detected. This procedure has been demonstrated using different singlet-NMR methods for high-resolution NMR spectroscopy in liquids.[22–25] Proposed singlet techniques include the M2S (magnetization-to-singlet) experiment,[26,27] a sequence introduced by Sarkar et al,[28] SLIC (spin-lock induced crossing),[29] APSOC (adiabatic passage singlet order conversion)[23,30] and M2S-CSS (magnetization-to-singlet chemical shift scaling).[31] These sequences show a strong dependence on the coupling regime (strong, weak or intermediate), ie the relation of the chemical shift difference of the two involved spins to their electron-mediated (*J*-)coupling and/or the offset of the applied pulses. The introduction of the general-condition magnetization-to-singlet technique (gc-M2S) unifies the concepts of various singlet-NMR techniques in one single experiment, which does not depend on the offset within the excitation bandwidth of the applied pulses and efficiently populates singlet states in all coupling regimes.[25] The gc-M2S sequence contains a set of parameters that can be tuned to selectively pass the signal from specific spin pairs, while suppressing the signal from other spins. Such filtering properties provide a valuable tool for molecular identification in systems characterized by spectral crowding. Following these considerations, we predict the suitability of such an approach for in vivo imaging experiments.

In this article, we demonstrate that singlet states of endogenous substrates can be accessed in vivo and specifically used to filter metabolites against the proton-rich background in the brain. To accomplish this goal, we propose an MRS experiment to perform localized singlet-filtered MRS (SiFi-MRS). First, we demonstrate its functionality in vitro on phantoms of various relevant metabolites. Finally, we report SiFi-MRS of glutamate in the hippocampus of a living mouse. Undesired signals arising from water and other metabolites are thereby completely suppressed and only the singlet-filtered glutamate is observed in vivo. Our presented work paves the way for introduction of singlet states into preclinical and potentially clinical studies. It brings new opportunities to study diseases based on filtering metabolite signals. We expect that new contrast agents and contrast mechanisms based on the singlet phenomenon will become feasible in vivo.

2 | EXPERIMENTAL

2.1 | In vitro studies

In vitro studies were conducted on phantoms containing glutamate, glutamine, NAA and GSH.

2.1.1 | Sample preparation

All the samples were obtained from commercial providers and used without further purification: L-glutamic acid monosodium salt monohydrate (49,621, Sigma-Aldrich Chemie GmbH, Taufkirchen, Germany), L-glutamine (G3126, Sigma-Aldrich Chemie GmbH, Taufkirchen, Germany), N-acetyl-L-aspartic acid (00920, Sigma-Aldrich Chemie GmbH, Taufkirchen, Germany) and L-GSH reduced (G4251, Sigma-Aldrich Chemie GmbH, Taufkirchen, Germany).

The buffer solution was prepared by diluting a commercial preparation, GIBCO phosphate-buffered saline (PBS) pH 7.4 10× (70011044, Thermo Fisher Scientific, USA), with ultrapure water. The buffer composition after dilution was KH_2PO_4 1.06 mM, NaCl 155 mM and Na_2HPO_4-$7H_2O$ 2.97 mM.

For each of the four compounds, 100 mM PBS stock solutions were prepared. Using ultrapure water, the following samples were prepared: (1) a mixture of glutamate, glutamine, NAA AND GSH at 20 mM each and (2) four 20 mM solutions, one for each of the considered compounds.

For each sample, the pH was adjusted to 7.3 ± 0.1 at 23 °C, as measured by a calibrated pH meter (HI9124, Hanna Instruments, Woonsocket, USA), using concentrated NaOH and/or HCl.

Five phantoms, one for each of the single compounds and one for the mixture, were prepared by completely filling standard 10 mm NMR tubes (Boroeco-10-7, Deutero GmbH, Kastellaun, Germany).

2.1.2 | MRI system

All in vitro experiments were conducted on a Bruker (Ettlingen, Germany) MRI system composed by an actively shielded superconducting wide-bore 7 T vertical magnet, in combination with a NEO console coupled to a GREAT 3-axis 60A gradient amplifier system. The controlling software was Paravision360 (Bruker, Ettlingen, Germany). For excitation and detection of the spins a room-temperature quadrature ^{1}H-transmit-receive volume resonator was used (RF coil size ≈ 25 × 50 mm^2) embedded within a MICWB40 gradient coil system (Bruker, Ettlingen, Germany). All experiments were conducted at room temperature.

2.1.3 | Experiments

In the gc-M2S sequence (see Figure 1; explained in Section 3), all the pulses were used at a nutation frequency of 2500 Hz (nominal RF amplifier output power = 1 W). 90° pulses were implemented as single block pulses of duration p_{90} =0.1 ms. 180° pulses were implemented as composite block pulses of the form $180^{\circ}_{\phi} \rightarrow \left(\frac{2}{3}p_{90}\right)_{\phi+\pi}\left(\frac{10}{3}p_{90}\right)_{\phi}\left(\frac{2}{3}p_{90}\right)_{\phi+\pi}$, where the phases of the pulses are expressed in radians. For the point resolved spectroscopy (PRESS) module, all the pulses and gradient parameters were defined by the controlling software as functions of the voxel size/geometry and reference power.

All spectra were acquired with 4096 points and a 14 ppm spectral window. Each spectrum is the average of 256 scans, preceded by eight dummy scans, with a repetition time of 5 s. T_{E1}/T_{E2} = 8 ms/7 ms were used for the PRESS module. A chemically selective saturation (CHESS)[36] module without outer volume suppression (OVS) was used for water suppression.

2.2 | Preclinical MRI studies

2.2.1 | MRI system

A preclinical actively shielded superconducting wide-bore 7 T MRI horizontal system was used for in vivo experiments (300 MHz ^{1}H Larmor frequency, BioSpec 70/20 USR, ParaVision 6.01, Bruker). For excitation and detection of the spins a cryogenic quadrature ^{1}H-transmit-receive mouse-head surface coil was used (26 K helium, RF coil size ≈ (20 × 27) mm^2, MRI CryoProbe, Bruker).

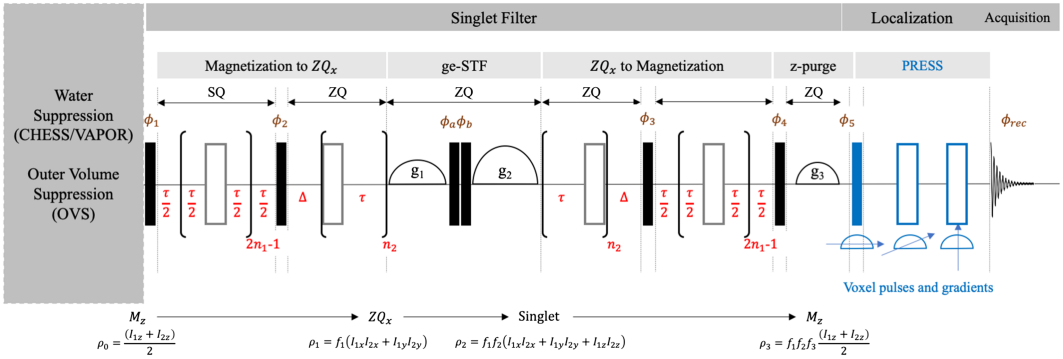

FIGURE 1 Sequence for localized SiFi-MRS. The sequence is used to acquire localized singlet-filtered NMR spectra. Filled and empty rectangles denote 90° and 180° pulses, respectively. Semicircles represent gradients: different sizes are used to stress that the accumulated integrated phases are linearly independent. The sequence consists of two main modules (filter and localization-acquisition) and one optional water/OVS module. The singlet filter module is partitioned in sub-blocks: magnetization is driven into two-spin order ZQ_x, then projected onto the singlet state by the ge-STF subblock, and finally ZQ_x is reported back into magnetization. The sequence parameters are the delay τ and Δ and the echo numbers, n_1 and n_2.The phases of the 90° pulses ϕ_1 and ϕ_2 are orthogonal; so are those of ϕ_3 and ϕ_4. Consecutive 180° pulses have alternating phases. The ge-STF works on a four-step phase cycle, as discussed in the main text

2.2.2 | Adjustments

The resonator was tuned and matched manually. After positioning the animal or test object, the homogeneity of the static magnetic field was adjusted by non-localized first-order shimming for MRI and by second-order shimming localized to the investigated $7 \times 2 \times 3$ mm^3 voxel selected for the spectroscopy. The vendor's standard routines were used (Bruker).

2.2.3 | Preclinical ^{1}H MRI images

For anatomical reference ^{1}H MRI was acquired. A multi-slice fast low-angle shot (FLASH) sequence was recorded to select the volume of interest for localized spectroscopy (10°, FOV (3×3) cm^2, matrix 256^2, in-plane resolution (117×117) μm^2, slice thickness 1 mm, slice distance 2 mm, T_R = 100 ms, T_E = 2.5 ms, acquisition time 583 s). In addition, MRI of three orthogonal slices was acquired with a T_2-weighted rapid acquisition with relaxation enhancement (RARE) sequence[33] (see Figure 3A-3D later; 90/180°, FOV (2×2) cm^2, matrix 256^2, in-plane resolution (78×78) μm^2, slice thickness 750 μm, T_R = 10 s, T_E = 33 ms, acquisition time 320 s).

2.2.4 | Preclinical PRESS and localization module

Localized spectroscopy was performed using PRESS[34] (parameters 90/180/180°, RF bandwidth 5400/2400/2400 Hz, voxel $7 \times 2 \times 3$ mm^3, T_R = 3.8 s, T_E = 20 ms, 256 scans, 2048 points, spectral bandwidth 5000 Hz, acquisition time ~16 min). Water and OVS were added to the sequence (VAPOR, bandwidth 200 Hz, duration 648.5 ms; OVS, slice thickness 5 mm, gap to voxel 0.5 mm). Note that SiFi-MRS was implemented based on this PRESS sequence with identical parameters and suppression schemes. However, in the singlet module ^{1}H block pulses were used with 200 μs pulse length for a 90° block pulse. Higher and lower flip angles were achieved by adjusting the pulse length.

2.2.5 | In vivo animal experiments

A mouse was used for the in vivo experiment (C57BL/6 strain, male, ≈1 year old, (35 ± 2) g; ordered from a commercial breeder and housed in an in-house experimental animal facility; three animals per type 2 cage) and was examined under narcosis (0.8-2% isoflurane in 0.8-1 L/min O_2 during spontaneous breathing; Vapor 2000, Dräger, Germany). It was placed head first in supine position on a custom-made animal bed to allow the brain to be placed close to the surface coil. The animal holder featured a water circulation system to maintain the body temperature of the animal at approximately 36.4-37 °C during the examination (1P T12184, Thermo Fisher Scientific). The respiration rate was maintained at around 60-120 breaths/min by adjusting the isoflurane dose, using a pressure sensitive cushion placed underneath the animal and a specialized monitoring device (SA Instruments 1030, Stony Brook, NY, USA).

The animal experiment was approved by the responsible local committee (Regierungspräsidium Freiburg; reference number 35-9185.81/G-19/162). All efforts were made to minimize suffering of the rodent. The examination was performed under isoflurane narcosis and animal physiology was continuously monitored throughout the experiment. We complied with the ARRIVE guidelines and report the completed ARRIVE guideline checklist in the supporting information.

3 | RESULTS

3.1 | Theory

In this paragraph, we introduce and briefly discuss the sequence used to perform localized SiFi-MRS. The overall scheme of the sequence is depicted in Figure 1. The pulse sequence consists of three modules, each performing a specific task. First, an optional water suppression module is used to reduce the large solvent signal, which may hinder the observation of metabolites at much lower concentrations. Secondly, the singlet filter module is designed to pass the signal of interest selectively. Finally, the localization block introduces spatial selectivity for the acquired NMR signal. Here, the PRESS method[34] was used to localize the region of interest.

For the description of the singlet filter module, we will consider systems of spin ½ only. The module is designed to filter the signal originating from selected spin pairs by transferring the longitudinal magnetization $M_z = I_{1z}+I_{2z}$ into zero-quantum (ZQ) order $ZQ_x = 2(I_{1x}I_{2x}+I_{1y}I_{2y})$, and after projection onto isotropic spin order (singlet state) back to magnetization M_z. The module is based on the gc-M2S sequence, which is able to access

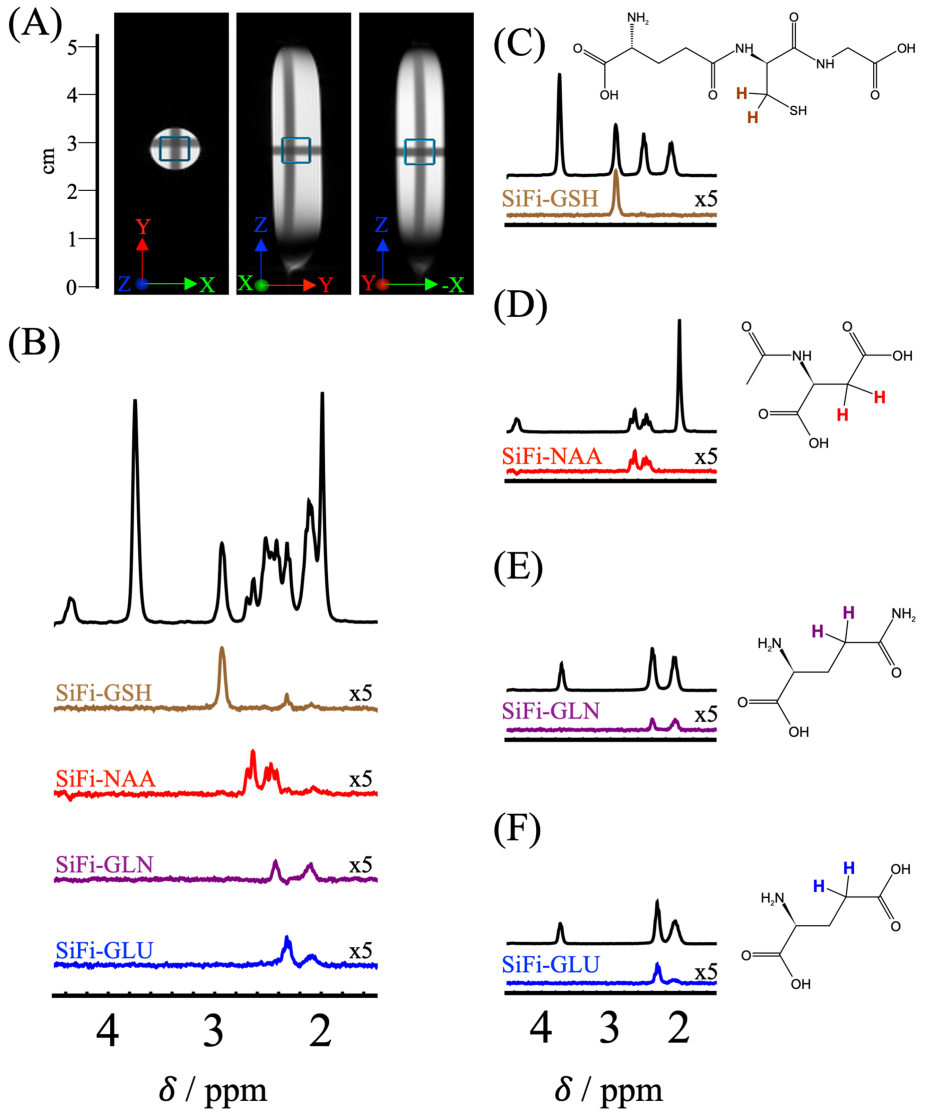

FIGURE 2 Localized SiFi-MRS of metabolites in vitro at 7 T. A, Orthogonal projections of a FLASH image of a typical phantom (10 mm NMR tube filled with PBS solution) used to demonstrate SiFi-MRS. The blue squares represent the 5 mm sides of the cubic voxel selected for localized spectroscopy in the subsequent panels. B, The localized ^{1}H MRS of a phantom containing a solution of 20 mM of the following: Glutamate (GLU), glutamine (GLN), NAA and GSH in PBS at pH = 7.4. The PRESS spectrum is shown at the top (black line) above a set of singlet filtered spectra for the specific metabolites, each acquired with the parameters given in the rows of Table 1, to select the spin pair of interest. C-F, The localized ^{1}H MRS spectra of 20 mM PBS solution for each of the compounds in separate phantoms: PRESS spectra (black) are shifted above the corresponding singlet filtered spectra. Beside each panel, the molecular structure of the corresponding compound is shown and the spin pair of interest is highlighted in the respective color. For clarity only the spectral region of interest is shown. The full frequency domain spectra are shown in the supporting information. The average chemical shifts of the non-exchangeable ^{1}H resonances are given in ppm, rounded to the closest multiple of 0.01: Glu-Hα = 3.74, Glu-Hβ = 2.08, Glu-Hγ = 2.34; Gln-Hα = 3.75, Gln-Hβ = 2.12, Gln-Hγ = 2.44; NAA-Asp-Hα = 4.38, NAA-Asp-Hβ = 2.58; GSH-Gly-Hα = 3.77; GSH-Glu-Hα = 3.77, GSH-Glu-Hβ = 2.15, GSH-Glu-Hγ = 2.54; GSH-Cys-Hα = 4.56, GSH-Cys-Hβ = 2.95

singlet states in the strong, intermediate and weak coupling regimes.[25] The gc-M2S sequence operates via consecutive single-quantum (SQ) and ZQ sub-blocks according to the following scheme:

$$I_{1z}+I_{2z} \overset{M_z \text{ to } ZQ_x}{\rightarrow} f_1 2(I_{1x}I_{2x}+I_{1y}I_{2y})+\ldots \overset{ge-STF}{\rightarrow} f_1 f_2 2(I_{1x}I_{2x}+I_{1y}I_{2y}+I_{1z}I_{2z})+\ldots \overset{ZQ_x \text{ to } M_z}{\rightarrow} f_1 f_2 f_3 (I_{1z}+I_{2z})+\ldots. \quad (1)$$

In Equation 1, $f_{1,2,3}$ indicate the partial transfer efficiencies of the sequences. The mathematical boundaries for the efficiencies are $0 \le |f_1|,|f_3| \le 1$ and $0 \le |f_2| \le \frac{2}{3}$. This means that about 66% of the initial magnetization is detectable at most after applying the filter. In general, the maximum

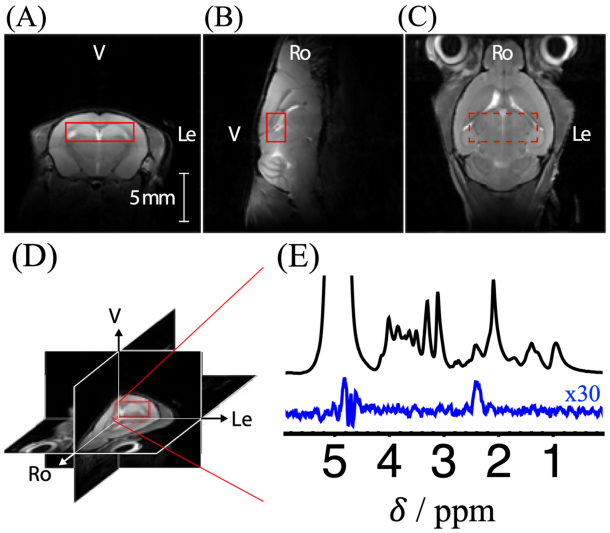

FIGURE 3 SiFi-MRS in vivo. A-D, Axial (A), sagittal (B) and coronal (C) MRI and their 3D projection (D) showing the voxel selected for spectroscopy (red square). This $7 \times 2 \times 3$ mm^3 region of interest is mostly covered by both hemispheres of the hippocampus. The coordinates in the MRI system correspond to V—ventral, Ro—rostral, Le—left. E, Top, PRESS ^{1}H MRS; bottom, localized SiFi-MRS of glutamate in vivo. Only glutamate is observed and all other resonances are suppressed. The SiFi spectrum was acquired with 256 scans within about 16 min

global transfer efficiency *f*is lower than 66% because the spin density matrix spreads into undesired operators at the intermediate steps, represented by dots in the expressions in Equation 1. Following the concepts of spherical tensor operator (STO) analysis,[35] the singlet projector is implemented as a set of two 90° pulses with phases ϕ_a and ϕ_b (Reference 32) flanked by two linearly independent gradients as in Reference 27. The use of gradients allows us to obtain high operator purity in short and simple phase cycles. In the analysis of gradient enhanced spherical tensor filters (ge-STFs), only longitudinal STOs $T_{l,0}$ need to be considered, as non-axial STOs are dephased by the gradients. In this paper, we used a four-step phase cycle with phases $\phi_a = 0$ and $\phi_b = \left\{\arccos\left[\frac{1}{15}\left(5 \pm 2\sqrt{5}\right)\right], \arccos\left[\frac{1}{15}\left(5 \pm 2\sqrt{5}\right)\right] + \pi\right\}$ so that (a) all odd-l $T_{l,0}$ are cancelled and (b) $T_{0,0}$ is preserved while the next two non-null operators are $T_{6,0}$ (scaled by a factor ~0.25) and $T_{10,0}$ (scaled by a factor ~0.2); see supporting information for details. In spin-½ systems, the maximum supported STO rank coincides with the number of spins. Many interesting metabolites contain groups of five or fewer connected proton nuclear spins, and further complicated phase cycles are not required.

By design, the singlet filter module will remove the signal from isolated magnetic equivalent groups of one or more spins, notably that from water. However, pulse imperfections, hardware related artifacts such as residual eddy currents and non-linear effects (radiation damping) can result in uncomplete water suppression. Water suppression below the noise level is achieved with the assistance of specialized modules. To this end, a CHESS-based water suppression scheme[36] can be used alone or in combination with OVS.

3.2 | Simulations

The sequence (Figure 1; explained in more detail in Section 3) parameters and the efficiencies reported in Table 1 were calculated in the following way. For each spin system, the liquid state spin Hamiltonian was built using the parameters reported by Govindaraju et al.[37] To represent pulses an RF Hamiltonian was added to the free evolution Hamiltonian. For each element of the singlet filter module shown in Figure 1, the propagator was obtained by exponentiation of the corresponding spin Hamiltonian. Gradients were simulated as projectors over the ZQ coherence subspace followed by a delay of 0.35 ms in the ge-STF block and 2 ms in the *z*-purge block. For a given parameter set $\{\tau, \Delta, n_1, n_2\}$, the initial spin operator, $\rho_0 = \sum_{i=1}^{N} I_{iz}$ (longitudinal magnetization summed over all the *N* spins in the spin system), was propagated over the sequence, including the *z*-purge

TABLE 1 Sequence parameters for the investigated metabolites. The efficiency *f* is calculated as the fraction of magnetization on the spin pair of interest that is passed through the singlet filter. The calculations were done as described in Section 3.2 using a nutation frequency of 2.5 kHz for all the pulses. $n_1$and n_2 represent the numbers of echoes in the SQ and ZQ blocks respectively, τ represents the inter-pulse delay in the echoes and Δ is the ZQ free evolution delay; see Figure 1

Parameters				Efficiency *f*/%			
n_1	n_2	τ /ms	Δ /ms	Glu H_γ	Gln H_γ	NAA H_β	GSH-Cys H_β
2	3	31.5	14.0	29.1	3.0	1.4	2.0
2	0	29.5	7.0	0.8	9.9	2.3	0.6
2	2	7.5	15.0	0.6	0.0	22.7	0.6
3	1	27.5	2.0	2.8	0.6	1.0	57.6

block. The final operator was averaged over four simulations with phases $\phi_1 = \phi_4 = \frac{\pi}{2}$, $\phi_2 = \phi_3 = 0$, $\phi_a = 0$ and $\phi_b = \left\{\arccos\left[\frac{1}{15}\left(5 \pm 2\sqrt{5}\right)\right], \arccos\left[\frac{1}{15}\left(5 \pm 2\sqrt{5}\right)\right] + \pi\right\}$, $\bar{\rho}_3 = \frac{\sum_{s=1}^{4}\rho_{3s}}{4}$. The efficiency of the singlet filter was calculated as the amplitude of the magnetization of the spin pair of interest, $I_{1z}+I_{2z}$, in $\bar{\rho}_3$ as

$$f = \frac{\left|\langle (I_{1z} + I_{2z})_3 \rangle\right|}{\|(I_{1z} + I_{2z})\|^2} \tag{2}$$

where the angular brackets $\langle | \rangle$ represent the scalar product and $\|\|$ represents the operator norm in the Hilbert space of operators (Liouville space).

All the 90° pulses were simulated as block pulses of duration p_{90} and all the 180°_{ϕ} pulses as composite block pulses $\left(\frac{2}{3}p_{90}\right)_{\phi+\pi}\left(\frac{10}{3}p_{90}\right)_{\phi}\left(\frac{2}{3}p_{90}\right)_{\phi+\pi}$.

For the values reported in able 1, p_{90} was set to 0.1 ms and the nutation frequency to 2500 Hz. For each spin system, the parameters were scanned according to the following scheme [initial:final:increment] units:

$$n_1 = [1:3:1]$$

$$n_2 = [0:4:1]$$

$$\tau = [1:50:0.5]\ \text{ms}$$

$$\Delta = [1:60:1.0]\ \text{ms}.$$

All calculations were performed in Wolfram Mathematica, Version 12.[38]

3.3 | In vitro experiments

In order to demonstrate the feasibility of our approach, we first conducted in vitro studies on the following molecules: glutamate, glutamine, NAA and GSH. These molecules play important roles in many physiological processes of living organisms, especially in the brains of animals. Glutamate is the main excitatory neurotransmitter in the central nervous system and doubles its role as metabolite by entering in the biosynthesis of many other molecules in the brain.[39] Glutamine has a vital role in regulating the concentration of glutamate and is the main transporter of amino nitrogen in the brain.[40] NAA is a main actor in the biochemistry of the central nervous system, where it serves multiple roles.[41] GSH is a well recognized antioxidant in living cells, defending reactive molecules against oxidative damage. Relative and absolute variations in the concentration of these metabolites have been associated with brain pathologies, including cancer and degenerative conditions.[39–41]

Localized in vitro ^{1}H MRS of the listed metabolites is shown in Figure 2, where A represents the phantom image with the localization region of 5 × 5 × 5 mm^3 indicated. Figure 2B displays the localized spectra for a mixture of all four metabolites, all at the same 20 mM concentration. The ^{1}H PRESS spectrum (top curve in black) is exemplary of the spectral overlap encountered in animal brains. Localized ^{1}H PRESS spectra for each of the metabolites, at 20 mM concentration, are shown in C-F. Singlet states can be effectively excited in the terminal proton pairs (H_γ in glutamate, glutamine and H_β in NAA and in GSH-Cys), which resonate in the region between 2 and 3 ppm, using the parameters given in Table 1. The parameters were obtained simulating the evolution of magnetization in the gc-M2S sequence under coherent spin dynamics for the full spin system of each metabolite at 7 T magnetic field; see Section 3.2 for details. We used these sets of parameters to acquire the localized singlet filtered images of phantoms shown in Figure 2. For each metabolite it is possible to filter the signal of a selected spin pair, while suppressing the NMR signal from other spins in the same molecule (C, D) or in other molecules in the mixture (B). For example, H_γ in glutamate can be observed selectively while H_γ in GSH-glutamate are suppressed. Similarly, H_γ in glutamate and in glutamine can be filtered individually by choosing appropriate parameters, despite having very similar spin couplings.

3.4 | In vivo experiments

The above obtained results encouraged us to perform localized SiFi-MRS in vivo studies. To this end, we have investigated a wild-type mouse within a 7 T preclinical MRI system and aimed to observe glutamate, an important neurotransmitter in the brain. In Figure 3A-3D we show the image of the mouse brain and localize the region of the hippocampus within a voxel of 7 × 2 × 3 mm^3. Figure 3E shows the regular PRESS ^{1}H image of the metabolites in the brain at the top. Once the singlet filter is applied, only the resonance of glutamate is detected, as shown in

figure 3E at the bottom. All other resonances from the proton background including water are suppressed. This proves first that singlet states can be populated in vivo even in endogenous metabolites, and second that our method can be used to filter out metabolite signals to investigate the brain. Finally, we note that all experiments were performed with a surface coil for excitation and detection. Although such a probe comes with an inherent B_1 inhomogeneity, we successfully populated singlet states, further demonstrating the robustness of our approach; see also Figures S1, S2 and S3 in the supporting information.

4 | DISCUSSION

In this article, we have introduced a filtered MRS experiment based on the phenomenon of nuclear spin singlet states and demonstrated its viability in vivo.

Signal filtration is achieved by maneuvering the magnetization of specific spin pairs through isotropic spin state order. The application of the sequence results in a net in-phase magnetization signal for the selected spin pair, which acts as a fingerprint for the metabolite of interest. High signal selectivity is achieved by tailoring the sequence timings and number to the intra-pair couplings as well as to other spins in the molecules. Relative contrast in ^{1}H MRS is increased by the concomitant suppression of other interfering signals that do not pass though the singlet filter, including that from water. The NMR experiment works for general coupling conditions between two spins 1/2, and hence includes the whole range from weakly to strongly coupled spins. By design the sequence is offset independent, and hence is robust with respect to the static (B_0) as well as RF (B_1) magnetic field inhomogeneities. All these aspects are particularly important for in vivo applications. In combination with localization modules, our experiment allows for spectroscopic imaging of specific regions of a sample or an organism.

We expect that the sequence can be effective at isolating metabolites of interest, especially in high field systems, where inhomogeneity and overlapping effects may still hinder their observation despite the increase in dispersion and signal intensity. In larger animals and humans, the possibility to use larger voxels compared with those used in our preclinical study (42 μL) should allow the observation of metabolites present at lower concentrations than glutamate. Once implemented on an MRI scanner, the use of the singlet sequence does not require any special equipment or further post-processing routines.

A possible limitation arises from the signal losses induced by intrinsic relaxation mechanisms, affecting SQ and ZQ modes during the duration of the sequence, which is of the order of 100 ms for the metabolites used in this study. However, inhomogeneity related losses are reduced by the use of 180° refocusing pulses.

Editing methods enhance the contrast of some metabolites by suppressing others (and the background). Singlet filters belong to the class of coherence filter methods and perform very well in this respect. Other powerful methods for spectrally filtered MRS are known, such as chemical exchange saturation transfer (CEST)[42] and *J*-editing methods such as Meshcher-Garwood point resolved spectroscopy (MEGA-PRESS).[43,44] CEST is limited to detecting molecules with exchangeable protons, as it makes use of frequency-selective saturation of the magnetization of a proton, which then exchanges with water and gives rise to signal attenuation. A challenge of the method is the strong spectral overlap of the ^{1}H MR signals: exchanging protons from different substances that have a similar chemical shift are difficult to separate. Similar to our SiFi approach, MEGA-PRESS exploits the known intramolecular *J*-couplings, ie that applying an RF pulse to one coupled spin can modify the time evolution of the coupling partner. Spectra are acquired with and without such editing to remove other, non-edited signals; the edit-off acquisition contains the full spectral information of all metabolites. The MEGA technique can be augmented with Hadamard encoding for simultaneous quantification of several *J*-coupled metabolites from a single measurement.[45,46] The possibility of effective coediting multiple metabolites using the singlet filter is envisaged, but its discussion remains outside the scope of this work and will be pursued in the future.

A key finding of our work is that singlet states of endogenous substrates can be accessed in vivo. As proof, we have used the singlet phenomenon to specifically observe glutamate in the hippocampus of a living mouse. Following this observation, we propose to use singlet states as probes for physiological processes in vivo. SiFi-MRS holds the potential of identifying new phenomena in diseases, as the lifetimes of singlet states are affected differently by the surroundings than the commonly used relaxation times T_1 and T_2. We are planning to investigate this in the future. Moreover, we foresee that many contrast agents based on hyperpolarized singlet states can be investigated in vivo. This will allow us to probe physiological function with maximized sensitivity over long periods of time (minutes to hours) exceeding the limitation of current contrast agents.

ACKNOWLEDGEMENTS

SM and SG acknowledge generous support by the Max Planck Society. Support by the German Consortium for Translational Cancer Research (DKTK) is gratefully acknowledged. The authors would like to thank Dr Jochen Leupold (Freiburg) for helping with the MRI implementation of the SiFi-MRS sequence. Open access funding enabled and organized by Projekt DEAL.

ORCID

Stefan Glöggler https://orcid.org/0000-0003-3354-6141

REFERENCES

1. Tkac I, Oz G, Adriany G, Ugurbil K, Gruetter R. In vivo ^{1}H NMR spectroscopy of the human brain at high magnetic fields: metabolite quantification at 4T vs. 7T. *Magn Reson Med*. 2009;62(4):868-879.
2. Shemesh N, Rosenberg JT, Dumez JN, Muniz JA, Grant SC, Frydman L. Metabolic properties in stroked rats revealed by relaxation-enhanced magnetic resonance spectroscopy at ultrahigh fields. *Nat Commun*. 2014;5(4958):1-8.
3. de Graaf RA, Rothman DL, Behar KL. High resolution NMR spectroscopy of rat brain in vivo through indirect zero-quantum-coherence detection. *J Magn Reson*. 2007;187(2):320-326.
4. Harris AD, Saleh MG, Edden RAE. Edited ^{1}H magnetic resonance spectroscopy in vivo: methods and metabolites. *Magn Reson Med*. 2017;77(4):1377-1389.
5. Choi C, Coupland NJ, Bhardwaj PP, Malykhin N, Gheorghiu D, Allen PS. Measurement of brain glutamate and glutamine by spectrally-selective refocusing at 3 tesla. *Magn Reson Med*. 2006;55(5):997-1005.
6. An L, Araneta MF, Johnson C, Shen J. Simultaneous measurement of glutamate, glutamine, GABA, and glutathione by spectral editing without subtraction. *Magn Reson Med*. 2018;80(5):1776-1786.
7. An L, Li SZ, Murdoch JB, Araneta MF, Johnson C, Shen J. Detection of glutamate, glutamine, and glutathione by radiofrequency suppression and echo time optimization at 7 Tesla. *Magn Reson Med*. 2015;73(2):451-458.
8. Carravetta M, Levitt MH. Long-lived nuclear spin states in high-field solution NMR. *J Am Chem Soc*. 2004;126(20):6228-6229.
9. Pileio G. Relaxation theory of nuclear singlet states in two spin-1/2 systems. *Prog Nucl Magn Reson Spectrosc*. 2010;56(3):217-231.
10. Theis T, Ortiz GX, Logan AWJ, et al. Direct and cost-efficient hyperpolarization of long-lived nuclear spin states on universal N-15(2)-diazirine molecular tags. *Sci Adv*. 2016;2(3):1-7.
11. Warren WS, Jenista E, Branca RT, Chen X. Increasing hyperpolarized spin lifetimes through true singlet eigenstates. *Science*. 2009;323(5922):1711-1714.
12. Vasos PR, Comment A, Sarkar R, et al. Long-lived states to sustain hyperpolarized magnetization. *Proc Natl Acad Sci USA*. 2009;106(44):18469-18473.
13. Bowers CR, Weitekamp DP. Transformation of symmetrization order to nuclear-spin magnetization by chemical-reaction and nuclear-magnetic-resonance. *Phys Rev Lett*. 1986;57(21):2645-2648.
14. Ardenkjaer-Larsen JH, Fridlund B, Gram A, et al. Increase in signal-to-noise ratio of > 10,000 times in liquid-state NMR. *Proc Natl Acad Sci USA*. 2003;100(18):10158-10163.
15. Adams RW, Aguilar JA, Atkinson KD, et al. Reversible interactions with para-hydrogen enhance NMR sensitivity by polarization transfer. *Science*. 2009;323(5922):1708-1711.
16. Kohler SJ, Yen Y, Wolber J, et al. In vivo ^{13}carbon metabolic imaging at 3T with hyperpolarized ^{13}C-1-pyruvate. *Magn Reson Med*. 2007;58(1):65-69.
17. Day SE, Kettunen MI, Gallagher FA, et al. Detecting tumor response to treatment using hyperpolarized ^{13}C magnetic resonance imaging and spectroscopy. *Nat Med*. 2007;13(11):1382-1387.
18. Nelson SJ, Kurhanewicz J, Vigneron DB, et al. Metabolic imaging of patients with prostate cancer using hyperpolarized [1-^{13}C]pyruvate. *Sci Transl Med*. 2013;5(198):198ra108-1-198ra108-10.
19. Grist JT, McLean MA, Riemer F, et al. Quantifying normal human brain metabolism using hyperpolarized [1-^{13}C] pyruvate and magnetic resonance imaging. *NeuroImage*. 2019;189:171-179.
20. Stevanato G, Hill-Cousins JT, Hakansson P, et al. A nuclear singlet lifetime of more than one hour in room-temperature solution. *Angew Chem Int Ed*. 2015;54(12):3740-3743.
21. Pileio G, Dumez JN, Pop IA, Hill-Cousins JT, Brown RCD. Real-space imaging of macroscopic diffusion and slow flow by singlet tagging MRI. *J Magn Reson*. 2015;252:130-134.
22. DeVience SJ, Walsworth RL, Rosen MS. Nuclear spin singlet states as a contrast mechanism for NMR spectroscopy. *NMR Biomed*. 2013;26(10):1204-1212.
23. Kiryutin AS, Pravdivtsev AN, Yurkovskaya AV, Vieth HM, Ivanov KL. Nuclear spin singlet order selection by adiabatically ramped RF fields. *J Phys Chem B*. 2016;120(46):11978-11986.
24. Mamone S, Gloggler S. Nuclear spin singlet states as magnetic on/off probes in self-assembling systems. *Phys Chem Chem Phys*. 2018;20(35):22463-22467.
25. Mamone S, Rezaei-Ghaleh N, Opazo F, Griesinger C, Gloggler S. Singlet-filtered NMR spectroscopy. *Sci Adv*. 2020;6(8):1-6, eaaz1955.
26. Pileio G, Carravetta M, Levitt MH. Storage of nuclear magnetization as long-lived singlet order in low magnetic field. *Proc Natl Acad Sci USA*. 2010;107(40):17135-17139.
27. Tayler MCD, Levitt MH. Singlet nuclear magnetic resonance of nearly-equivalent spins. *Phys Chem Chem Phys*. 2011;13(13):5556-5560.
28. Sarkar R, Vasos PR, Bodenhausen G. Singlet-state exchange NMR spectroscopy for the study of very slow dynamic processes. *J Am Chem Soc*. 2007;129(2):328-334.
29. DeVience SJ, Walsworth RL, Rosen MS. Preparation of nuclear spin singlet states using spin-lock induced crossing. *Phys Rev Lett*. 2013;111(17):1-5, 173002.
30. Pravdivtsev AN, Kiryutin AS, Yurkovskaya AV, Vieth HM, Ivanov KL. Robust conversion of singlet spin order in coupled spin-1/2 pairs by adiabatically ramped RF-fields. *J Magn Reson*. 2016;273:56-64.
31. Kharkov B, Duan XY, Tovar ES, Canary JW, Jerschow A. Singlet excitation in the intermediate magnetic equivalence regime and field-dependent study of singlet-triplet leakage. *Phys Chem Chem Phys*. 2019;21(5):2595-2600.
32. Pileio G, Levitt MH. Isotropic filtering using polyhedral phase cycles: application to singlet state NMR. *J Magn Reson*. 2008;191(1):148-155.
33. Hennig J, Nauerth A, Friedburg H. RARE imaging: a fast imaging method for clinical MR. *Magn Reson Med*. 1986;3(6):823-833.
34. Bottomley PA. Spatial localization in NMR spectroscopy in vivo. *Ann N Y Acad Sci*. 1987;508:333-348.
35. van Beek JD, Carravetta M, Antonioli GC, Levitt MH. Spherical tensor analysis of nuclear magnetic resonance signals. *J Chem Phys*. 2005;122(24):1-5, 244510.
36. Haase A, Frahm J, Hanicke W, Matthaei D. ^{1}H NMR chemical shift selective (CHESS) imaging. *Phys Med Biol*. 1985;30(4):341-344.
37. Govindaraju V, Young K, Maudsley AA. Proton NMR chemical shifts and coupling constants for brain metabolites. *NMR Biomed*. 2000;13(3):129-153.
38. Mathematica [computer program]. *Version 12.1*. Champaign, IL: Wolfram; 2020.

39. Shen J. Chapter 2.4—Glutamate. In: Stagg C, Rothman D, eds. *Magnetic Resonance Spectroscopy*. San Diego, CA: Academic; 2014:111-121.
40. Ross BD. Biochemical considerations in ^{1}H spectroscopy. Glutamate and glutamine; *Myo*-inositol and related metabolites. *NMR Biomed.* 1991;4(2):59-63.
41. Moffett JR, Ross B, Arun P, Madhavarao CN, Namboodiri AM. *N*-Acetylaspartate in the CNS: from neurodiagnostics to neurobiology. *Prog Neurobiol.* 2007;81(2):89-131.
42. Jones KM, Pollard AC, Pagel MD. Clinical applications of chemical exchange saturation transfer (CEST) MRI. *J Magn Reson Imaging.* 2018;47(1):11-27.
43. Mescher M, Merkle H, Kirsch J, Garwood M, Gruetter R. Simultaneous in vivo spectral editing and water suppression. *NMR Biomed.* 1998;11(6):266-272.
44. Puts NAJ, Edden RAE. In vivo magnetic resonance spectroscopy of GABA: a methodological review. *Prog Nucl Magn Reson Spectrosc.* 2012;60:29-41.
45. Chan KL, Puts NAJ, Schar M, Barker PB, Edden RAE. HERMES: Hadamard Encoding and Reconstruction of MEGA-Edited Spectroscopy. *Magn Reson Med.* 2016;76(1):11-19.
46. Oeltzschner G, Saleh MG, Rimbault D, et al. Advanced Hadamard-encoded editing of seven low-concentration brain metabolites: principles of HERCULES. *NeuroImage.* 2019;185:181-190.

SUPPORTING INFORMATION

Additional supporting information may be found online in the Supporting Information section at the end of this article.

How to cite this article: Mamone S, Schmidt AB, Schwaderlapp N, et al. Localized singlet-filtered MRS in vivo. *NMR in Biomedicine*. 2020; e4400. https://doi.org/10.1002/nbm.4400